

Sb-intercalated layered double hydroxides–poly(vinyl chloride) nanocomposites: Preparation, characterization, and thermal stability

Shu-Ting Liu, Ping-Ping Zhang, Kang-Kang Yan, Yuan-Hu Zhang, Ying Ye, Xue-Gang Chen

Ocean College, Zhejiang University, Hangzhou 310058, People's Republic of China

Correspondence to: X.-G. Chen (E-mail: chenxg83@zju.edu.cn)

ABSTRACT: In this study, a novel SbS_3^{3-} -intercalated layered double hydroxide (Sb-LDH) was prepared by simultaneous recovering of LDH structures and intercalation of SbS_3^{3-} into LDH layers. The prepared Sb-LDH composites remain the hydroxide structure with layered geometry and show higher thermal property than that of LDH. When applied to poly(vinyl chloride) (PVC) composites, Sb-LDH showed limited thermal stability for PVC at the early stage of thermal and thermooxidative degradation processes. However, Sb-LDH could retard the thermal cracking of the carbonaceous conjugated polyene of PVC which may hinder further degradation, and the moderate amount of Sb-LDH (1, 2, and 5 wt %) in PVC resin can retard the process of decarbonation and enhance char formation. Sb-LDH also promoted the transparency of PVC but darkened the color. With the advantages of transparency promotion, high temperature resistance, and long-term stability, the prepared Sb-LDH is a potential thermal stabilizer for PVC resins. © 2015 Wiley Periodicals, Inc. *J. Appl. Polym. Sci.* **2015**, *132*, 42524.

KEYWORDS: clay; poly(vinyl chloride); properties and characterization; thermal properties

Received 22 February 2015; accepted 20 May 2015

DOI: 10.1002/app.42524

INTRODUCTION

Poly(vinyl chloride) (PVC) is a commercial thermoplastic that was used in various industrial fields such as building materials, electrical wire and cable insulation, floor coverings, and so on. However, PVC exhibits poor thermal stability when exposed to heat by giving off hydrochloric acid (HCl) that in turn accelerates the degradation process.¹ Therefore, many researchers are motivated to develop various thermal stabilizers for PVC. At present, the commonly used stabilizers are lead salts, metal soaps, and organotin compound.^{2–4} Lead salts exhibit long-term thermal stability and can react with hydrogen chloride, and thus retard the further degradation process caused by eliminated HCl.⁵ Metal soaps can scavenge HCl and exchange the labile chlorine, and therefore are extensively used in combination with other stabilizers for their good transparency and lubricity for plastic.^{6,7} Organotin compound acts as an efficient stabilizer through effective absorption of HCl and introduction of stable ester group to intervene in the radical degradation process.⁸ Although these stabilizers are highly efficient, the applications are still constrained by some of the disadvantages of toxicity, environmental pollution, and high cost.^{9,10} Developing an environmental friendly stabilizer with low cost is still a global concern.

Layered double hydroxides (LDHs) are a class of anionic clays with layered structure. The general formula of LDHs is

$[\text{M}_1^{2+}_x\text{M}_2^{3+}_y(\text{OH})_z][\text{A}^{n-}]_x/n \cdot z\text{H}_2\text{O}$, where M_1^{2+} and M_2^{3+} represent divalent and trivalent metal cations in brucite-like layers, respectively, and A^{n-} is the non-framework charge compensating inorganic or organic anion.¹¹ Due to its high versatility, easy tailoring, and low cost, LDHs are promising materials for many practical applications in catalysis, adsorption, electrochemistry, pharmaceuticals, and so on.^{12,13} LDHs also possess the capacity of HCl absorption which make them potential for application as PVC thermal stabilizer.¹⁴ In addition, LDHs have relatively weak interlayer bonding and consequently present expanding properties through the intercalation of different anions.^{15,16} Therefore, many researchers have investigated the LDHs intercalated by other functional anions as thermal stabilizers for PVC. Lin *et al.* reported that MgAl-CO₃-LDH and MgZnAl-CO₃-LDH can enhance the thermal stability of PVC in terms of both long-term stability and early coloring.⁹ Zhang *et al.* prepared the 2-hydroxy-4-methoxybenzophenone-5-sulfonic acid anion-intercalated Mg-Al-carbonated layered double hydroxide (LDH-BP) and investigated its thermal stabilization of PVC. The results turned out that LDH-BP could not only scatter the incident light but also absorb the released HCl, which improves the resistance of PVC to both accelerated weathering and thermal degradation.¹⁷ In our previous work, thermal stability of LDH/NaSb(OH)₆ nanocomposite and Mg-Al LDH nanolayers for PVC has been studied.⁷ The results showed that both LDH/NaSb(OH)₆ and Mg-Al LDH could

enhance the thermal stability of PVC resin and LDH/NaSb(OH)₆ composites showed relatively higher initial stability and long-term stability than that of Mg-Al LDH.

In this work, we intercalated SbS₃³⁻ ions into the interlayers of LDHs and prepared a novel LDH-SbS₃ nanocomposite (Sb-LDH), which is characterized by XRD, SEM, IR techniques, thermogravimetric analysis (TGA), and differential thermal analysis (DTA). When applied as thermal stabilizers for PVC resins, we evaluated the thermal stability and thermal properties of Sb-LDH/PVC composites.

EXPERIMENTAL

Materials

Mg-Al LDH was obtained from Jiangsu Ruijia Chemistry (Yixing, China). Stibnite (99.8 wt % Sb₂S₃) was purchased from Xikuangshan Mining Bureau (Loudi, China). Na₂S, paraffin, diisooctyl phthalate (DIOP), and stearic acid were supplied by Sinopharm Chemical Reagent (Shanghai, China). Unstabilized PVC with K-value of 71–72 was obtained from Aladdin (Shanghai, China). All chemicals were used as received without further purification.

Preparation of Sb₂S₃-Intercalated LDHs

In a typical procedure, 50 g powdered stibnite (99.8 wt % Sb₂S₃) with a diameter of less than 150 μm was added into 500 mL of 8% Na₂S solutions and stirred for 2 h to ensure sufficient reaction. The mixture solution was filtered to remove insoluble residues and diluted for 3–4 times. Calcination (550°C for 5 h) product of Mg-Al LDH (150 g) was added into the diluted filtrate with pH of 8–9 and stirred at 90°C for 2 h. The obtained precipitate was filtered, washed thoroughly by deionized water, and dried at 90°C, Sb-LDH was prepared.

Preparation of Sb-LDH/PVC Composites

All compositions (40 g PVC, 24 g DIOP, 0.2 g paraffin, 0.2 g stearic acid, and certain amounts of Sb-LDH) were melt compounded using a two-roll mill at 165°C for 5 min. The obtained product was then molded into sheets with thickness of 2 mm using a laboratory press at 165°C and 14 MPa for 5 min. According to the mass percent of Sb-LDH added to PVC, the obtained Sb-LDH/PVC composites were named as Sb-LDH-1 (1 wt %, 0.4 g), Sb-LDH-2 (2 wt %, 0.8 g), Sb-LDH-5 (5 wt %, 2 g), Sb-LDH-10 (10 wt %, 4 g), and Sb-LDH-20 (20 wt %, 8 g).

Characterizations

The elemental contents of Sb-LDH were examined by an INCA Energy X-ray energy spectrometer (EDS, Oxford). The structure of samples was characterized by a D/max 2550 X-ray diffractometer (Rigaku, Japan) with Cu Kα radiation ($\lambda = 0.15406$ nm) at a scan rate of 0.02°·s⁻¹. The surface morphology was observed by an Utral 55 Field Emission Scanning Electronic Microscope (FE-SEM, CorleisD, Germany).

The thermal stability of PVC resin and Sb-LDH/PVC composites was determined by thermal aging test and TGA. The thermal aging test has been carried out by adding 1 × 1 cm strips into a thermal aging test box at 180 ± 1°C according to ISO standard 305–1990.¹⁸ TGA and DTA experiments were conducted on a DTG-60A (Shi-

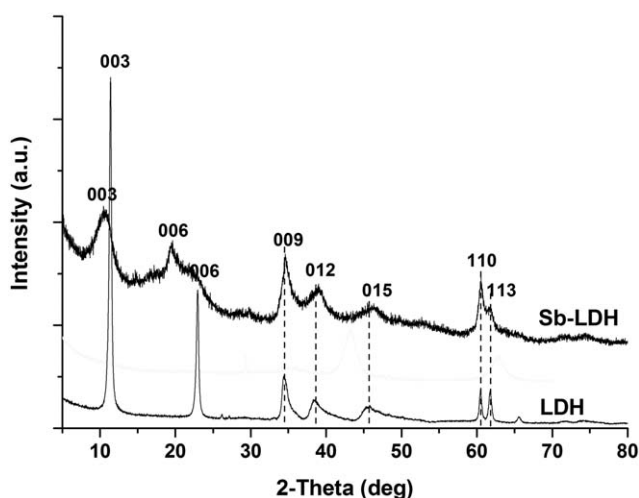


Figure 1. X-ray diffraction (XRD) patterns of LDH and Sb-LDH.

mazu, Japan) automatic Thermal Analyzer with a heating rate of 10°C min⁻¹ under air atmosphere.

RESULTS AND DISCUSSION

XRD Patterns

The XRD spectra of LDH and synthesized Sb-LDH are shown in Figure 1. Sb-LDH exhibited common features and similar characteristic diffraction peaks as original LDH indicating hydroxyl structure with layered geometry. According to the position of the basal peak (003), the interlayer spacing of LDH is 0.777 nm, which is conform to those previously reported in the literature.^{7,19,20} After intercalated by SbS₃³⁻, the diffraction peak of (003) shifted to lower 2θ values; correspondingly, the *d*-spacing value (*d*₀₀₃) of the prepared Sb-LDH was increased from 0.777 to 0.866 nm. The results suggest that the SbS₃³⁻ have been successfully intercalated into the interlayer of LDH. In addition, the basal peaks of (003) and (006) were broadened after intercalation, attributed to the reduced crystallinity during the calcination and rehydration processes.^{21,22}

SEM Characterizations

The morphology of LDH and Sb-LDH (right) revealed by SEM are shown in Figure 2. Most particles of LDH are nearly hexagonal and presented plate-like shape with obvious edges indicating the layered structure. The average diameter of LDH is around 45.8 nm according to SEM images. Sb-LDH revealed relatively uniform flakes with comparable smooth edges, which is consistent with the XRD result that Sb-LDH exhibited lower degree of crystallinity. Comparing the morphology of LDH and Sb-LDH, the average diameter of the Sb-LDH with 339.8 nm is significantly larger than that of LDH, while the thickness of Sb-LDH is lower than that of LDH.

IR Characterizations

The FT-IR spectra of LDH and Sb-LDH (Figure 3) were recorded to investigate their vibrations in the octahedral lattice, the hydroxyl group, and interlayer anions. For both samples, the broad bands between 3400 and 3500 cm⁻¹ in the IR spectra are attributed to the stretching mode of hydrogen-bonded hydroxyl groups.²³ The band around 1638 cm⁻¹ may be

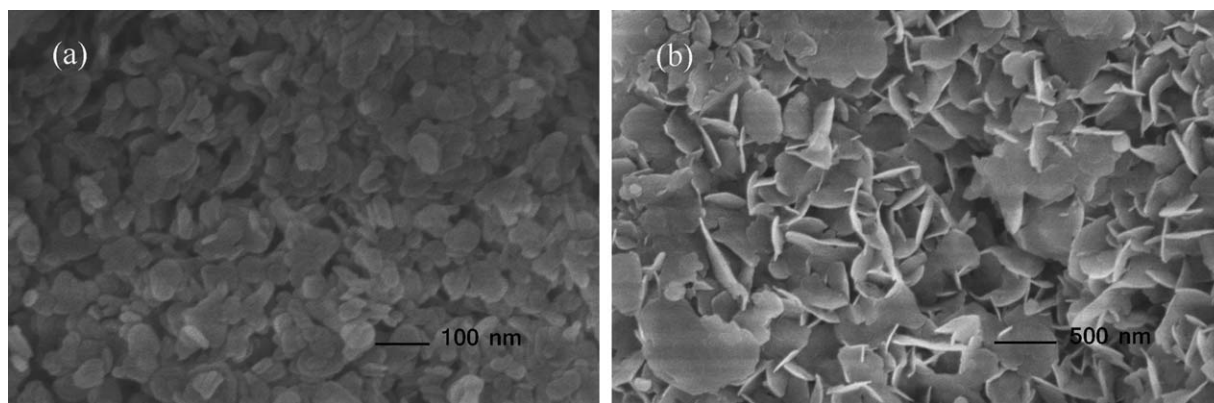


Figure 2. SEM images of prepared (a) LDH and (b) Sb-LDH.

associated to the vibration mode δ_{OH} from interlayer water.²⁴ An intense absorption peak around 1370 cm^{-1} is assigned to the ν_3 vibration mode of interlayer carbonate.^{25,26} The peaks corresponding to Al–O and Mg–O stretching modes in the brucite layer appear at 650 and 418 cm^{-1} , respectively.²⁷ For the absorption peak at 1370 cm^{-1} , Sb-LDH represents weaker intensity comparing to LDH due to the substitution of carbonate by SbS_3^{3-} . It is imperative to note that two new absorption peaks of 1125 and 999 cm^{-1} revealed in Sb-LDH is corresponding to $\text{Na}_2\text{S}_2\text{O}_3$, which is generated by the oxidation of a fraction of Na_2S during preparation process.²⁸ Since the absorption peaks of Sb–S stretching mode and S–Sb–S stretching mode are below 350 cm^{-1} , which exceeds the measurement range of present, no characteristic absorption peaks of SbS_3^{3-} can be observed in the Sb-LDH's IR spectra.²⁹

Thermal Properties of LDH and Sb-LDH

Figure 4 shows the TG and DTG curves of LDH and Sb-LDH in air. The weight losses of both samples include two stages. The first stage, below 220°C , was due to the loss of surface and interstitial water,³⁰ where the temperature of maximum decreasing rate (T_{max}) of LDH and Sb-LDH were 205°C with 14% weight loss and 201°C with 11% weight loss, respectively. At the

second decomposition stage with the temperature that started at above 250°C , both carbon dioxide and water from the dehydroxylation were lost. In addition, SbS_3^{3-} was oxidized and generated Sb_2O_5 with SO_2 emission, which retarded the weight loss of Sb-LDH. As a result, the weight loss of LDH was 22.46 wt % while that of Sb-LDH was only 16.24 wt %. The maximum decreasing rate of weight loss exhibited at 381°C for LDH and 447°C for Sb-LDH. By comparing the TG curves of LDH and Sb-LDH, the major steps and trends of weight loss are similar, suggesting that Sb-LDH exhibits similar composition and structure to that of LDH. For the DTG curves, however, the T_{max} of both LDH and Sb-LDH are almost identical at stage one, while Sb-LDH presented much higher T_{max} values than that of LDH at stage two. This may be ascribed to the lower amount of decarbonation of Sb-LDH, because a fraction of CO_3^{2-} was intercalated by SbS_3^{3-} and the oxidation temperature of Sb-LDH to generate SO_2 is higher than that of CO_2 . In addition, the residual content of Sb-LDH (57.92%) at 800°C was higher than that of LDH (53.91%), which further confirmed the introduction of SbS_3^{3-} into LDH.

Color and Transparence of PVC Composites

The effect of Sb-LDH on the color and transparence of PVC composites was investigated and is shown in Figure 5. It can be seen that the colors of all Sb-LDH/PVC samples are generally darker than that of PVC resin without any additive, indicating

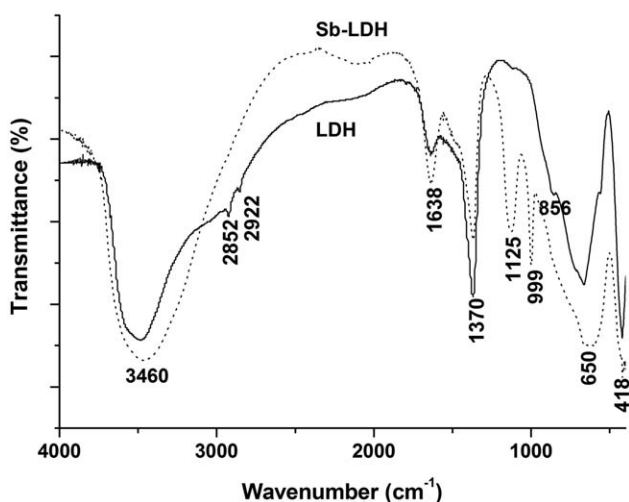


Figure 3. FTIR spectra of LDH and Sb-LDH.

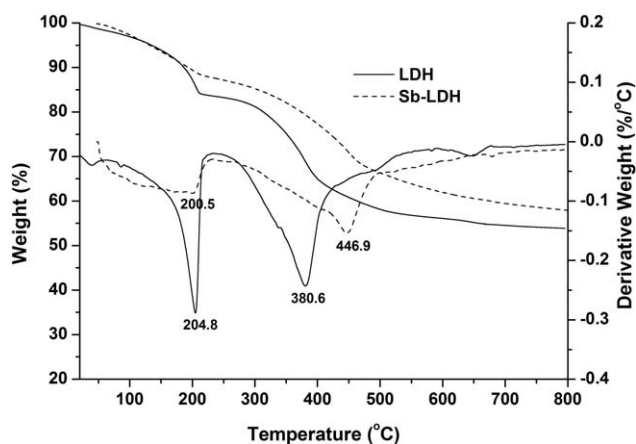


Figure 4. TG and DTG curves of LDH and Sb-LDH.

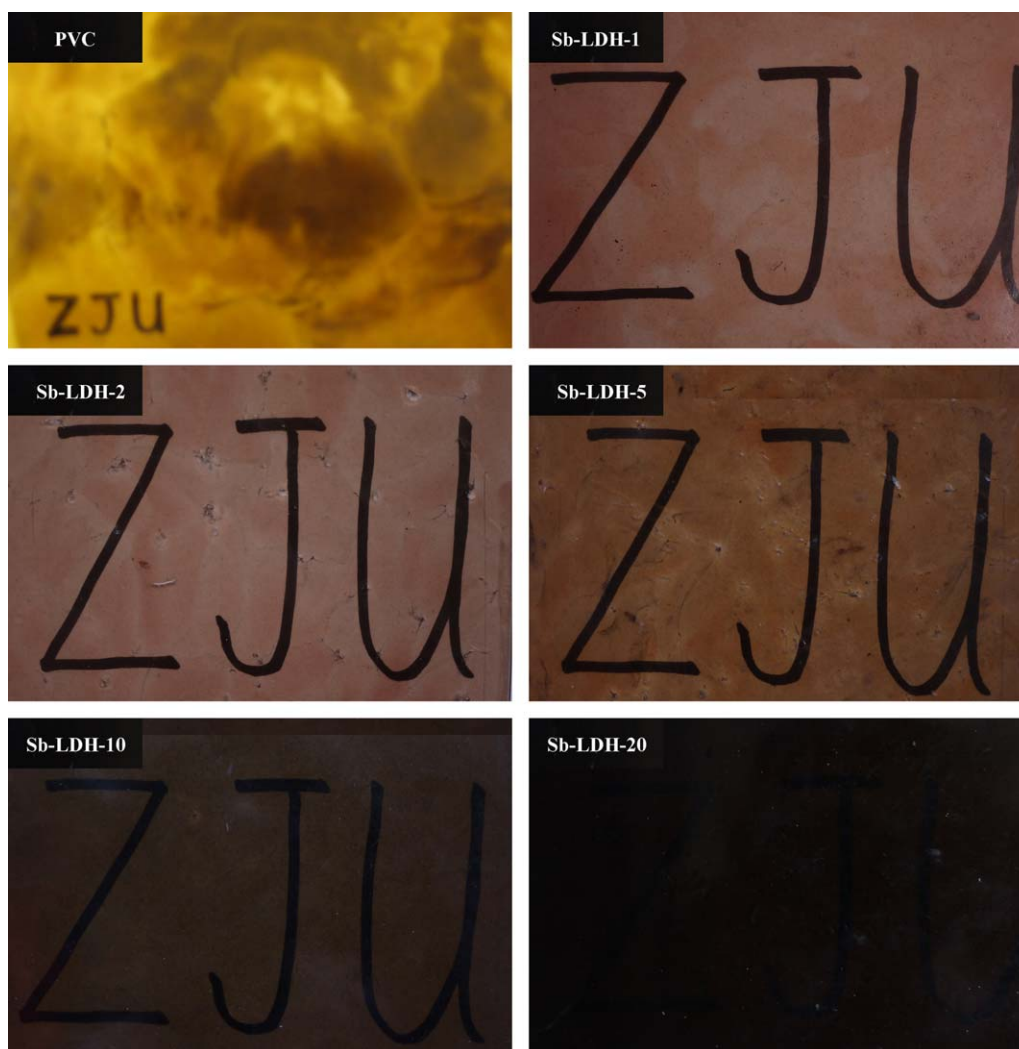


Figure 5. Photos of PVC resins and Sb-LDH/PVC composites with thickness of 2 mm. The PVC resins cover a white paper with black letters of “ZJU” drawing by a marker pen. The photos are taken by Panasonic GF3 mirror less camera. [Color figure can be viewed in the online issue, which is available at wileyonlinelibrary.com.]

that Sb-LDH has no positive contribution to the lower color degree of plastics. It is ascribed to the impact of the original color of Sb-LDH, which is dark grey. Therefore, the color of Sb-LDH/PVC darkens with the increasing of Sb-LDH loading and eventually exhibited a dark gray when 20 wt % Sb-LDH was added. However, Sb-LDH will improve the transparency of PVC at loadings of lower than 5%. There are probably two main reasons accounting for the transparency improvement.^{31–33} First, the refractive index of Sb-LDH nearly matches that of PVC, which is able to hinder the light scattering. Second, Sb-LDH has good compatibility with PVC resin, leading to strong interfacial adhesion between Sb-LDH and PVC. Thereby, the agglomeration of Sb-LDH and the formation of interphase boundary were prevented, resulting in the light scattering reduction. In conclusion, the addition of Sb-LDH will darken the color and improve the transparency for PVC, suggesting that Sb-LDH may be suitable for some deep-colored plastic materials to improve their transparency by adding appropriate amount of Sb-LDH.

Thermal Decomposition of PVC Composites

The TGA and DTA curves of PVC and Sb-LDH/PVC are shown in Figure 6. The TG curves for all samples exhibit a three-step weight loss in the range of 100–600°C. The first step occurred between 230 and 350°C, which is due to the autocatalytic dehydrochlorination of PVC, dehydration of Sb-LDH, and oxidation of DIOP. This process is also illustrated by DTA analysis in Figure 6(d), where the heat flow on the vertical axis basically presents the variation in reaction heat, exhibiting a strongest exothermic peak corresponding to the $T_{\max 1}$ (the temperature of maximum decreasing rate at first stage) at around 295°C for Sb-LDH/PVC and 306°C for PVC-resin. During the dehydrochlorination process of PVC, hydrogen chloride was liberated and a chromophoric-conjugated polyene structure was formed.³⁴ However, as can be seen in Figure 6(b), PVC resin decomposed in a broader and higher temperature range than Sb-LDH/PVC composites and the intensity of DTG peaks at $T_{\max 1}$ of Sb-LDH/PVC are stronger than that of PVC resin, which implies that Sb-LDH can accelerate the dehydrochlorination of PVC. The reason may

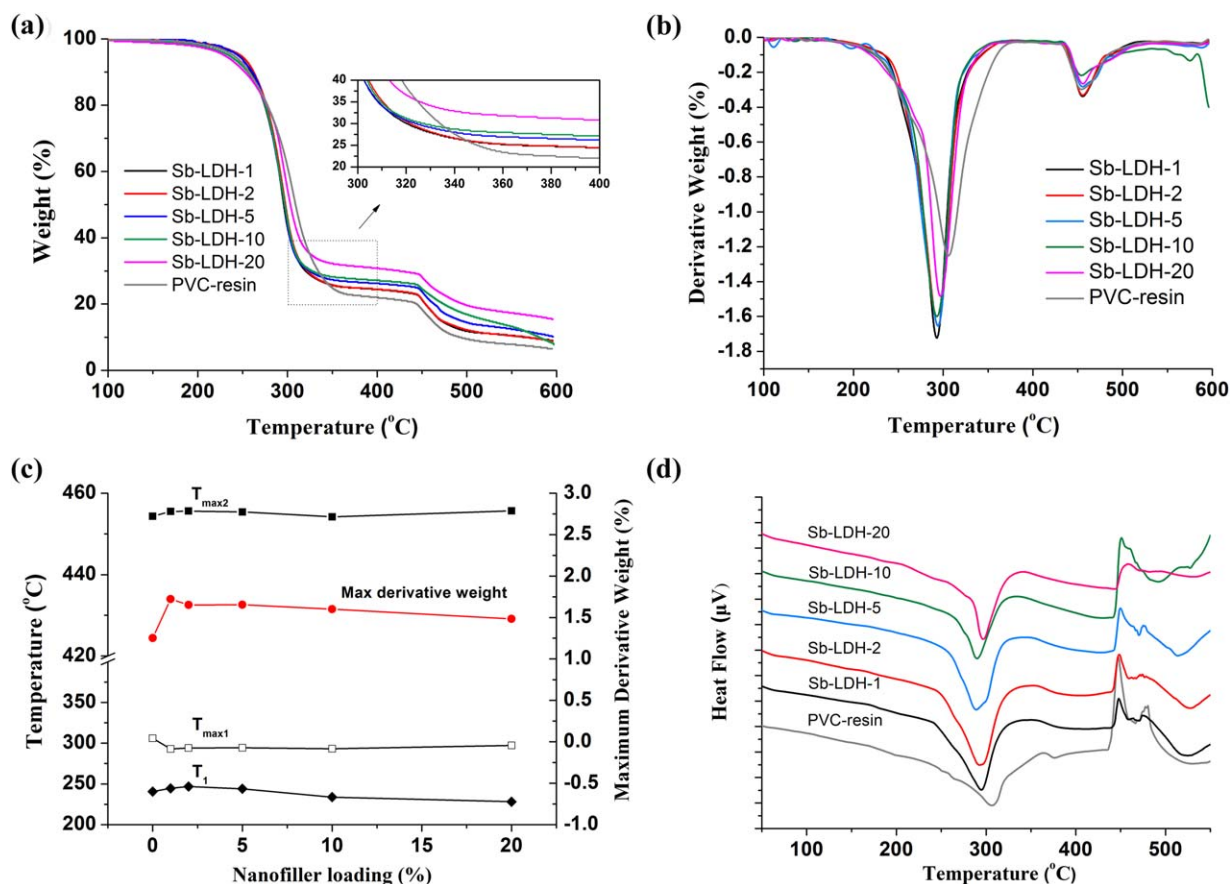


Figure 6. Effect of PVC and Sb-LDH/PVC on the thermal decomposition of PVC composites: (a) TGA curves of PVC and Sb-LDH/PVC; (b) DTG curves of PVC and Sb-LDH/PVC; (c) T_1 , T_{max1} , T_{max2} , and max derivative weight results of PVC and Sb-LDH/PVC; (d) DTA curves of PVC and Sb-LDH/PVC. [Color figure can be viewed in the online issue, which is available at wileyonlinelibrary.com.]

lie in that Sb-LDH absorbed some amount of released HCl during heating process, which in turn accelerates the HCl releasing at the first step.³⁵ As the temperature increased, the conjugated polyene structures were subjected to a combustion process with heat emitting, resulting in an exotherm peak at around 450 °C in DTA pattern at the second step weight loss, which is corresponding to the T_{max2} (the temperature of maximum decreasing rate at second stage) exhibiting in the DTG curves. The second weight loss involved the processes of dehydrocarbonation of PVC and both dehydroxylation and decarbonation of Sb-LDH according to previous TG results of Sb-LDH. The third weight loss step occurs in the range of 500–600 °C due to the continuous dehydrocarbonation and oxidation of PVC and its char-like materials.³⁶ As shown in Figure 6(a), the TGA curves of Sb-LDH/PVC is higher than that of PVC above 350 °C, implying that Sb-LDH could hinder the combustion process of carbonaceous conjugated polyene in the second stage and further degradation in the third stage to improve the thermal stability of PVC. In addition, since the TG examinations were carried out under air atmosphere, carbonaceous composition of PVC was combusted into carbon dioxide and the residue of pristine PVC at 600 °C was 6.56 wt %. Therefore, we can calculate the theoretical values of Sb-LDH/PVC residues at 600 °C according to the previous TG result of Sb-LDH via adding up the value that 6.56% multiply the weight of PVC

in Sb-LDH/PVC and the value that 61.95 wt % (residue of Sb-LDH at 600 °C) multiply the weight of Sb-LDH in Sb-LDH/PVC. As a result, the theoretical values of Sb-LDH-1/PVC, Sb-LDH-2/PVC, and Sb-LDH-5/PVC residue increase from 7.11 to 9.33 wt % with the nanofiller loading, which were lower than the measured values of 8.6–10.15 wt %, while the theoretical values of Sb-LDH-10/PVC and Sb-LDH-20/PVC were higher than that of measured values, revealing that the moderate amount (below 10 wt %) of Sb-LDH in PVC resin can retard the process of decarbonation and promote char formation.

The T_{max1} of Sb-LDH/PVC and PVC exhibited the values of around 295 and 306 °C, respectively. The initial decomposition temperature (T_1) of all samples increase slightly with the dosage of Sb-LDH at first; however, when the nanofiller loading was higher than 2 wt %, the T_1 started to decrease due to the promotion of the dehydrochlorination of PVC caused by Sb-LDH. The T_{max2} of Sb-LDH/PVC and PVC exhibited similar values at about 455 °C. However, as can be seen in Figure 6(d), the exotherm peak at around 450 °C of Sb-LDH/PVC on the DTA curve is weaker than that of the PVC-resin, which can be ascribed to the counteraction of endothermic reaction by the decomposition of Sb-LDH with its T_{max2} of 445 °C. Comparing to the thermal behavior of LDH/PVC in our previous work,⁷ Sb-LDH is

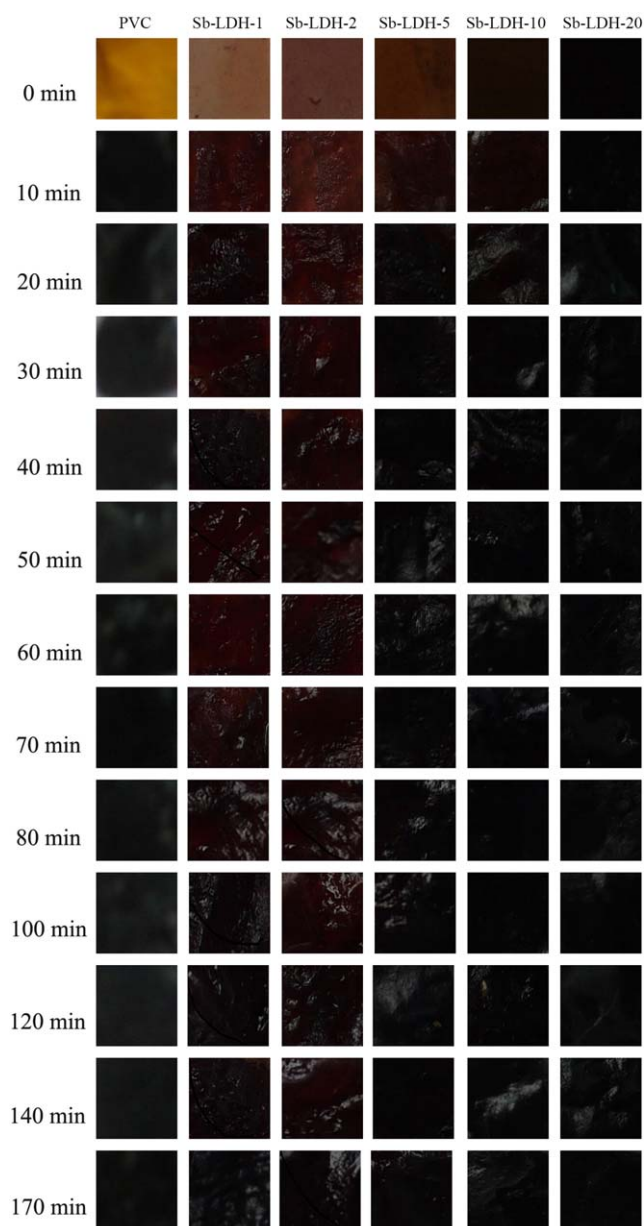


Figure 7. Thermal aging of PVC and Sb-LDH/PVC composites: (PVC) PVC resins without stabilizers added, (Sb-LDH-1, Sb-LDH-2, Sb-LDH-5, Sb-LDH-10, Sb-LDH-20) Sb-LDH/PVC composites. The photos are taken by Panasonic GF3 mirrorless camera. [Color figure can be viewed in the online issue, which is available at wileyonlinelibrary.com.]

not as efficient as LDH, especially at the first step to absorb released HCl. In general, Sb-LDH is more thermally stable to retard the thermal cracking of the carbonaceous conjugated polyene of PVC at the second and third steps, and the moderate amount of Sb-LDH (1, 2, and 5 wt %) in PVC resin can retard the process of decarbonation and enhance char formation.

Thermal Aging of PVC and Sb-LDH/PVC Composites

The thermal stability of PVC resin and Sb-LDH/PVC composites is shown in Figure 7. PVC resin without thermal stabilizer became completely black within just 10 min at $180 \pm 1^\circ\text{C}$. It can be observed in strips of Sb-LDH-1 and Sb-LDH-2, the color

change followed the sequence of brown–reddish brown–black. The reddish brown appeared at 10 min but was maintained until 80 min for Sb-LDH-1 and 100 min for Sb-LDH-2. This is because there are two steps for Sb-LDH to absorb HCl. First, HCl reacted with interlayer ions of Sb-LDH, which could produce H_2S gas result in the reddish brown within 10 min. Second, HCl absorbed by the LDH layer and formed metal chlorides, which enhance the thermal stability of PVC for more than 80 min. When the nanofiller increase to 5 wt %, the time of color change from reddish brown to black was shortened sharply in just 10 min, that is, the strip color of Sb-LDH-5 has completely become black within 30 min. It is attributed to the fact that more Sb-LDH introduced lead to more H_2S generated, which reduce the thermal stability of PVC. Since the initial strip color of Sb-LDH-10 and Sb-LDH-20 is black, it is hard to evaluate their thermal stability through color changes. Comparing to our previous work, both LDH/PVC and Sb-LDH/PVC exhibited better thermal stability at low concentrations, where the optimum amount of nanofiller loading is 1 wt % for LDH/PVC and 2 wt % for Sb-LDH/PVC. In addition, both LDH/PVC and Sb-LDH/PVC have little effect on the resistance to early coloring result in short time discoloration, which ascribed to the LDHs accelerated the dehydrochlorination at the beginning of the thermo-oxidative degradation. However, LDH/PVC presented lighter initial color and hence exhibited more color gradients from light brown to black, while Sb-LDH/PVC exhibited slower speed of color darkening from reddish brown to black, indicating that Sb-LDH/PVC have higher long-term stability than that of LDH/PVC.

CONCLUSIONS

In this research, we successfully prepared Sb-LDH by intercalation of SbS_3^{3-} into LDH layers and investigated the thermal stability of Sb-LDH/PVC with comparing to that of LDH/PVC in our previous work. The prepared Sb-LDH exhibited better thermal stability than that of pristine LDH. The maximum decreasing rate of weight loss exhibited at 381°C for LDH and 447°C for Sb-LDH. When applied to PVC composites, Sb-LDH can promote the transparency of PVC but darkened the color. For the effect of thermal stability enhancement on PVC, Sb-LDH would even accelerate the decomposition and coloring of PVC by producing H_2S gas at the early stage of thermal and thermo-oxidative degradation processes, while it can retard the thermal cracking of the carbonaceous-conjugated polyene of PVC to hinder further degradation at the second and third stages and the moderate addition of Sb-LDH (1, 2, and 5 wt %) in PVC resin could enhance char formation. The optimum amount of Sb-LDH addition is 2 wt % with optimal overall performance in transparency and thermal stability exhibiting in Sb-LDH-2/PVC. With the advantages of transparency promotion, high temperature resistance, and long-term stability, Sb-LDH is a promising thermal stabilizer for PVC, and also has the potential to combine with some short-term co-stabilizers for better thermal stability of PVC, which can be applied on some deep-colored materials, such as disc, sewer pipe, and oil pipeline.

ACKNOWLEDGMENTS

This research is supported by the “Fundamental Research Funds for the Central Universities,” the Ministry of Education, People’s Republic of China, Research Fund for the Doctoral Program of Higher Education of China (20110101120045), Zhejiang leading Team of SQT innovation (2010R5036), and National Natural Science Foundation of China (No. 41273022).

REFERENCES

1. Baum, B.; Wartman, L. H. *J. Appl. Polym. Sci.* **1958**, *28*, 537.
2. Markarian, J. *Plastics, Plast. Addit. Compd.* **2004**, *6*, 46.
3. Balköse, D.; Gökçel, H. İ.; Göktepe, S. E. *Eur. Polym. J.* **2001**, *37*, 1191.
4. Arkiş, E.; Balköse, D. *Polym. Degrad. Stab.* **2005**, *88*, 46.
5. Fox, V. W.; Hendricks, J. G.; Ratti, H. J. *Ind. Eng. Chem.* **1949**, *41*, 1774.
6. Liu, Y. B.; Liu, W. Q.; Hou, M. H. *Polym. Degrad. Stab.* **2007**, *92*, 1565.
7. Chen, X. G.; Wu, D. D.; Lv, S. S.; Zhang, L.; Ye, Y.; Cheng, J. P. *J. Appl. Polym. Sci.* **2010**, *116*, 1977.
8. Mohamed, N. A.; Sabaa, M. W.; Khalil, K. D.; Yassin, A. A. *Polym. Degrad. Stab.* **2001**, *72*, 53.
9. Lin, Y.; Wang, J.; Evans, D. G.; Li, D. *J. Phys. Chem. Solids* **2006**, *67*, 998.
10. Liu, J.; Chen, G.; Yang, J. *Polym.* **2008**, *49*, 3923.
11. Wang, Q.; O’Hare, D. *Chem. Rev.* **2012**, *112*, 4124.
12. Li, F.; Duan, X. Layered Double Hydroxides; Evans, D. G., Eds.; Struct Bond: Berlin, **2006**; Vol. 119, Chapter 4, pp 193.
13. Williams, G. R.; O’Hare, D. *J. Mater. Chem.* **2006**, *16*, 3065.
14. van der Ven, L.; van Gemert, M. L. M.; Batenburg, L. F.; Keern, J. J.; Gielgens, L. H.; Koster, T. P. M.; Fischer, H. R. *Appl. Clay Sci.* **2000**, *17*, 25.
15. Zhang, F. Z.; Xiang, X.; Li, F.; Duan, X. *Catal. Surv. Asia* **2008**, *12*, 253.
16. Roussel, H.; Briois, V.; Elkaim, E.; Roy, A. d.; Besse, J. P. *J. Phys. Chem. B* **2000**, *104*, 5915.
17. Zhang, X. F.; Zhou, L. C.; Pi, H.; Guo, S. Y.; Fu, J. W. *Polym. Degrad. Stab.* **2014**, *102*, 204.
18. Plastics: Determination of Thermal Stability of Poly(Vinyl Chloride) and Related Chlorine-Containing Homopolymers and Copolymers and Their Compounds - Discoloration Method, ISO 305-1990 (E).
19. Yuan, S.; Li, Y.; Zhang, Q.; Wang, H. *Colloids Surf. A* **2009**, *348*, 76.
20. Saber, O. *J. Mater. Sci.* **2007**, *42*, 9905.
21. Ni, Z. M.; Xia, S. J.; Wang, L. G.; Xing, F. F.; Pan, G. X. *J. Colloid Interface Sci.* **2007**, *316*, 284.
22. You, Y.; Zhao, H.; Vance, G. F. *Appl. Clay Sci.* **2002**, *21*, 217.
23. Cavani, F.; Trifirò, F.; Vaccari, A. *Catal. Today* **1991**, *11*, 173.
24. Allmann, R. *Chimia* **1970**, *24*, 99.
25. Goh, K. H.; Lim, T. T.; Dong, Z. *Water Res.* **2008**, *42*, 1343.
26. Carja, G.; Nakamura, R.; Aida, T.; Niiyama, H. *Microporous Mesoporous Mater.* **2001**, *47*, 275.
27. Lee, W. D.; Im, S. S.; Lim, H. M.; Kim, K. J. *Polym.* **2006**, *47*, 1364.
28. Miller, F. A.; Wilkins, C. H. *Anal. Chem.* **1952**, *24*, 1253.
29. Minceva-Sukarova, B.; Jovanovski, G.; Makreski, P.; Soptrajanov, B.; Griffith, W.; Willis, R.; Grzetic, I. *J. Mol. Struct.* **2003**, *651-653*, 181.
30. Bai, Z. M.; Wang, Z. Y.; Zhang, T. G.; Fu, F.; Yang, N. *Appl. Clay Sci.* **2012**, *59-60*, 36.
31. Huang, S.; Cen, X.; Zhu, H.; Yang, Z.; Yang, Y.; Tjiu, W. W.; Liu, T. *Mater. Chem. Phys.* **2011**, *130*, 890.
32. Zhou, C.; Chen, M.; Tan, Z. Y.; Sun, S. L.; Ao, Y. H.; Zhang, M. Y.; Yang, H. D.; Zhang, H. X. *Eur. Polym. J.* **2006**, *42*, 1811.
33. Gu, Z.; Liu, W.; Dou, W.; Tang, F. *Polym. Compos.* **2009**, *31*, 928.
34. Wu, C. H.; Chang, C. Y.; Hor, J. L.; Shih, S. M.; Chen, L. W.; Chang, F. W. *Can. J. Chem. Eng.* **1994**, *72*, 644.
35. Liu, J.; Chen, G.; Yang, J.; Ding, L. *J. Appl. Polym. Sci.* **2010**, *116*, 2058.
36. Xu, Z. P.; Saha, S. K.; Braterman, P. S.; D’Souza, N. *Polym. Degrad. Stab.* **2006**, *91*, 3237.